RESEARCH ARTICLE | NOVEMBER 04 2024

Borosilicate glass with low dielectric loss and low permittivity for 5G/6G electronic packaging applications

Rocio Rodriguez-Cano ; Nicholas L. Clark; John C. Mauro ; Michael T. Lanagan

AIP Advances 14, 115105 (2024)
https://doi.org/10.1063/5.0211061

Borosilicate glass with low dielectric loss and low permittivity for 5G/6G electronic packaging applications

Cite as: AIP Advances 14, 115105 (2024); doi: 10.1063/5.0211061
Submitted: 5 August 2024 • Accepted: 18 October 2024 •
Published Online: 4 November 2024

Rocio Rodriguez-Cano,[1,2,a] Nicholas L. Clark,[3] John C. Mauro,[3] and Michael T. Lanagan[1,4]

AFFILIATIONS

[1] Materials Research Institute, Penn State University, University Park, Pennsylvania 16802, USA
[2] Electronic Systems Department, APMS Section, Aalborg University, 9220 Aalborg East, Denmark
[3] Department of Materials Science and Engineering, Penn State University, University Park, Pennsylvania 16802, USA
[4] Department of Engineering Science and Mechanics, Penn State University, University Park, Pennsylvania 16802, USA

[a] Author to whom correspondence should be addressed: rrc@es.aau.dk

ABSTRACT

A phase-separated borosilicate glass, with a relative permittivity ranging from 3 to 3.5 and a loss tangent as low as 5.6×10^{-4}, is presented for packaging applications for the next generation of mobile communications. Ionic polarizability for each borosilicate composition was calculated from the Clausius–Mossotti relationship for both the vitreous and crystalline structures, and the polarizability difference between the two is proportional to the dielectric loss. Small amounts of alkali modifier were added to improve the glass processability, and the loss tangent increased to the $1–7 \times 10^{-3}$ range. The resulting glass is phase-separated, which has no impact in the millimeter-wave spectrum, as the wavelengths are considerably greater than the length scale of each immiscible phase.

I. INTRODUCTION

Over the past several decades, Moore's law has fueled integrating more computing capabilities onto single silicon chips, embodied in system-on-chip (SoC) designs. However, transistor costs are rapidly rising for sophisticated chips at advanced nodes, facing hurdles from technology complexity and manufacturing yield issues. These escalating costs for complex monolithic SoCs contrast the diverse performance, efficiency, and form factor demands of emerging workloads across artificial intelligence (AI), 5G, Internet-of-things (IoT), and automotive domains. System-on-package (SoP) architecturally separates specialized functions into modular chiplet blocks that are heterogeneously integrated onto a package. By mixing tailored pieces leveraging the most suitable process per purpose, system-on-package promises adaptable, cost-optimized scaling unconstrained by the limitations of any individual chip technology for the hardware needs of the future.[1,2] The full benefits of system-on-package integration hinge on innovating high-performance interposer materials and interfaces. Interposer materials present respective fabrication challenges and device-level trade-offs in power, thermal, and reliability parameters. Moreover, the incorporation of several frequency bands in the millimeter-wave (mm-wave) spectrum for the upcoming generations of communications has accentuated the challenge of increased propagation losses. Consequently, there is a growing emphasis on the exploration of materials with low loss to address this issue. In addition, low dielectric constant is also desired, as it facilitates faster propagation of the electromagnetic waves, given the inverse relationship between propagation speed and dielectric constant. Furthermore, lower relative permittivity contributes to a reduction in capacitive coupling between adjacent conductors.

Glass offers key advantages for millimeter wave system packaging, due to its low fabrication cost and high tunability properties.[3] With intrinsically low surface roughness, glass can enable fine lithographic patterning below 8 μm to fabricate dense signal features.[4] Through compositional tuning, glass thermal expansion traits can be matched with other package components for reliable long-term operation. Dimensional stability also proves superior on glass backing structures compared to organic substrates,[5] critical for high frequencies and tolerances in next-generation wireless modules. By

leveraging these useful optical and physical properties, glass interposers promise a high-performance pathway to integrate diverse functions such as antenna arrays into sophisticated multifunction millimeter wave electronic assemblies.

The dielectric properties of silicate glasses are linked to composition and structure. Key attributes such as oxygen coordination and bonding configurations can be tuned across glass processing conditions to customize polarization behaviors for electronics. This structure–property relationship allows designing glass compositions to precisely meet target dielectric performance specifications by defining local molecular arrangements, despite lacking long-range periodic order. Understanding the link between a material's molecular structure and its dielectric characteristics involves a crucial parameter known as ionic polarizability. The Clausius–Mossotti equation emerges as a valuable tool, enabling the estimation of a material's dielectric constant by incorporating the polarizability values of its constituent ions and its density,

$$\epsilon_r = \frac{3V_m + 8\pi\alpha_D^T}{3V_m - 4\pi\alpha_D^T}, \tag{1}$$

$$V_m = \frac{MW}{\rho N_A}, \tag{2}$$

where V_m is the molar volume (in $\mathring{A}^3$), α_D^T is the total dielectric polarizability, MW is the molecular weight, ρ is the glass density, and N_A is Avogadro's number.[6] A comprehensive compilation of polarizability data for various ions in crystalline materials was curated by Shannon in Ref. 7. Notably, boron stands out with the lowest recorded polarizability of 0.05 $\mathring{A}^3$, while silicon and oxygen exhibit values of 0.87 and 2.01 $\mathring{A}^3$, respectively. Typical glass modifiers, such as Li, Na, Mg, and Ca, possess polarizability values of 1.2, 1.8, 1.32, and 3.16 $\mathring{A}^3$, sequentially.

Research detailed in Ref. 6 showcases that the polarizability of ions in non-crystalline states surpasses that observed in corresponding crystalline states like quartz. This discrepancy in ionic polarizability between a material's crystalline and non-crystalline phases demonstrates a proportional relationship with the measured dielectric loss across a broad spectrum in the mm-wave bands. Using elements with lower polarizability allows us to decrease the loss difference between crystalline and glassy counterparts, therefore obtaining low loss glasses.

The search for materials with these properties is not something recent. Van Uitert *et al.*[8] proposed in 1973 a borosilicate glass for the cladding of optical fibers, as the cladding material needs to have a lower dielectric constant than the core material, fused silica in this case. The commercial glasses with the lowest reported relative permittivity are Corning Vycor[9] and SCHOTT 8325,[10] with values of 3.8 and 4, respectively. Vycor also has a low loss tangent of 7.2×10^{-4} at 10 GHz.

This paper introduces an innovative approach to design a glass by reducing its total polarizability, which leads to a silicate glass composition characterized by a high boron percentage. The choice of boron is strategic, leveraging its inherently low polarizability, coupled with the immiscibility of glass formers B_2O_3 and SiO_2.[11]

II. MATERIALS AND METHODS

Six glasses were synthesized with a range of compositions $xB_2O_3 \cdot (1-x)SiO_2$ mol, where $0.33 \le x < 1$. Bulk glass was prepared by manually mixing B_2O_3 and SiO_2 powders. 60-g batches were calcined at 200 °C for 1.5 h to prevent foaming in the mix due to excess water. After calcining, the batches were melted in a platinum–rhodium crucible at 1600 °C for 3 h using a traditional drop-down furnace. The samples were poured and pressed with a metallic plate to obtain two flat surfaces of at least 2.5 cm in diameter. This procedure was not always enough to ensure complete melting of the batch, particularly for the higher silica compositions. These compositions had large amounts of stones present after pouring. Therefore, the glass composition was measured using inductively coupled plasma atomic emission spectroscopy (ICP-AES).

In order to improve glass processability and its durability from corrosion, additional samples with a small percentage of alkali added to the borosilicate glass were synthesized using the same procedure. Due to the presence of alkali modifiers, these batches melted significantly better and were generally free of large stones. Three different alkali percentages were evaluated, 2%, 5%, and 10%. The alkalis employed were lithium, sodium, and potassium oxides. The ratio between boron and silicon has been kept constant (50% B–50% Si, which corresponds to 33% mol B_2O_3–67% mol SiO_2). Unlike the binary borosilicates, which were quenched at room temperature without annealing, the alkali-borosilicates were annealed overnight at 400 °C to avoid thermal shock. The annealing has been performed according to the boron's glass transition temperature, to guarantee that one phase is fully annealed. Phase-separation is affected by thermal history and could also affect the loss and polarizability, but this effect goes beyond the scope of this paper.

A. Characterization

The dielectric properties were measured using a split-cavity or resonant mode dielectrometer (RMD-C, GDK Product, Inc.), where a TE_{011} mode is excited. The samples were characterized right after pouring, to avoid any corrosion to their surface. After the measurement, they were kept under vacuum conditions. The authors would like to emphasize that the dielectric properties are bulk properties of a material and not a surface one. In addition, the surface layer represents a very small fraction of the overall sample thickness and the samples are very dense with no porosity. Therefore, the impact from possible hydration on the dielectric properties is negligible. For the broadband characterization of the materials, refer to Ref. 12 for details about the measurement techniques. Apart from the processed materials, the glasses AF45, OA-10G, BK7, and Borofloat 33 and fused silica JGS2 were also characterized. AF45, BK7, and Borofloat 33 are glasses produced by SCHOTT. OA-10G is obtained from Nippon Electric Glass Co. The densities of the samples were measured with a Mettler Toledo balance using the Archimedes principle. Inductively coupled plasma analysis was used to determine the stoichiometry of the compositions. The surface morphology of several samples was explored using scanning electron microscopy (SEM, Verios G4). The samples have been polished and coated with a 5 nm layer of iridium prior to imaging to reduce charging and

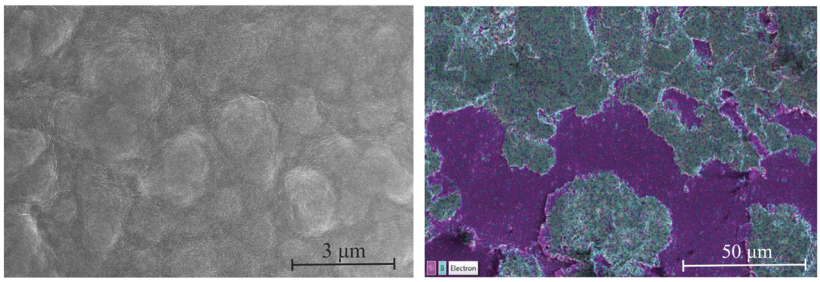

FIG. 1. (a) SEM image of a fracture surface of the 33% B_2O_3–67% SiO_2 composition. (b) EDS map of the 60% B_2O_3–40% SiO_2 composition. The silicon is shown in magenta, and the boron is shown in cyan.

improve the image quality. The fracture surfaces were also coated with a 5 nm iridium layer.

III. RESULTS

To achieve a low-loss glass, this paper explores the concept of minimizing the polarizability of the resulting material. As mentioned before, boron oxide has been chosen due to its exceptionally low polarizability compared to other elements. Incorporating B_2O_3 into a silica network can lead to phase separation in the final glass. To show this effect, a representative scanning electron microscopy (SEM) micrograph of a fracture surface of one of the proposed binary borosilicates is included in Fig. 1(a). To confirm that the darker areas in this figure corresponded to regions with different compositions, Fig. 1(b) shows an energy dispersive spectroscopy (EDS) map distinguishing boron and silicon. Phase separation is typically undesirable for most glass applications. The difference in refractive indices of the phases will often lead to opacity due to Rayleigh scattering. From a high-frequency electronics perspective, the wavelengths in the mm-wave spectrum are long enough (1 mm at 300 GHz) not to be scattered by the micrometer-scale silica droplets. Furthermore, the immiscible borosilicate glass can be treated as a composite where effective medium theory applies to quantify the dielectric properties. Figure 2 shows two manufactured samples with low and high boron content. Phase-separation is visible at plain sight in the sample with a lower boron content. The polariscopic inspection of Fig. 2(c) shows some residual thermal stress. As the glasses are phase-separated, it is not possible to completely remove all thermal stress, due to the difference in the expansion coefficient of the phases.

The dielectric properties of the unmodified borosilicates are detailed in Table I. The compositions with a higher boron amount can yield a dielectric constant of 3 and a loss tangent of 5.6×10^{-4}, while the ones with less boron have similar loss and a dielectric constant of 3.47. As mentioned previously, Vycor and SCHOTT 8325 are examples of glasses, which are considered to be low-loss and low dielectric constant, possessing losses of 7.2×10^{-4} and 2.1×10^{-3} and permittivities of 3.8 and 4, respectively. Fused silicas exhibit lower electrical losses compared to phase-separated borosilicate glasses. This difference might be attributed to the more uniform internal structure of fused silica, lacking the boron oxide phase or interfaces between boron-rich and silica-rich regions present in phase-separated borosilicate glass. These interfaces and separate phases can potentially increase the ionicity of the network, leading to higher losses in borosilicate glasses. The measured loss tangent for fused silica JGS2 is 1.6×10^{-4}, and the relative permittivity 3.86. The proposed borosilicates have the advantage of lower cost than fused silicas, as they melt at lower temperatures. These borosilicates have a lower dielectric constant and a similar loss tangent. The dielectric properties of various silicates were measured and are plotted in Fig. 3 across a wide frequency range. It can be seen that the dielectric constant of the proposed borosilicate is lower than that of any other silicate. Its loss tangent is around one order of magnitude lower than that of common glasses.

Table II presents the ICP analysis results for various samples. Due to the difference in melting temperatures between boron oxide and silica, volatilization of the boron oxide is expected. The last three samples indicate a volatility range of 2%–10% for boron oxide. However, the higher than anticipated mol percentage of boron oxide observed in the first sample cannot be attributed to inherent stoichiometric volatility. Instead, this discrepancy arises solely from incomplete processing. A significant portion of the silicon oxide remained unmelted within the crucible and, consequently, was not included in the final glass. This artificially increases the relativet

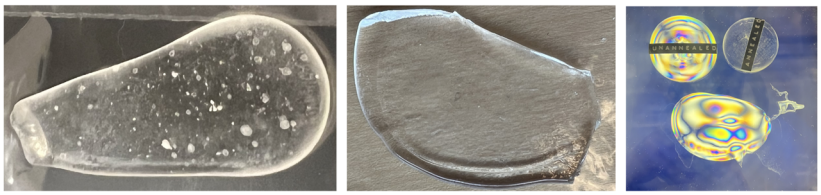

FIG. 2. (a) Manufactured 33% B_2O_3–67% SiO_2 sample. (b) Manufactured 90% B_2O_3–10% SiO_2 sample. The samples are ~10 cm long. (c) Polariscopic inspection of the 90% B_2O_3–10% SiO_2 sample. The two samples on top correspond to two unannealed and annealed glass references.

TABLE I. Dielectric properties of the proposed borosilicate glass compositions.

Composition (mol. %)	Permittivity	Loss tangent	Frequency (GHz)
33% B_2O_3–67% SiO_2	3.47	6.54×10^{-4}	11.57
50% B_2O_3–50% SiO_2	3.43	8.25×10^{-4}	14.82
60% B_2O_3–40% SiO_2	3.41	6.68×10^{-4}	12.22
67% B_2O_3–33% SiO_2	3.34	8.52×10^{-4}	14.24
80% B_2O_3–20% SiO_2	3.19	5.93×10^{-4}	13.02
90% B_2O_3–10% SiO_2	2.98	5.62×10^{-4}	12.77
100% B_2O_3–0% SiO_2	3.20	1.20×10^{-3}	13.47

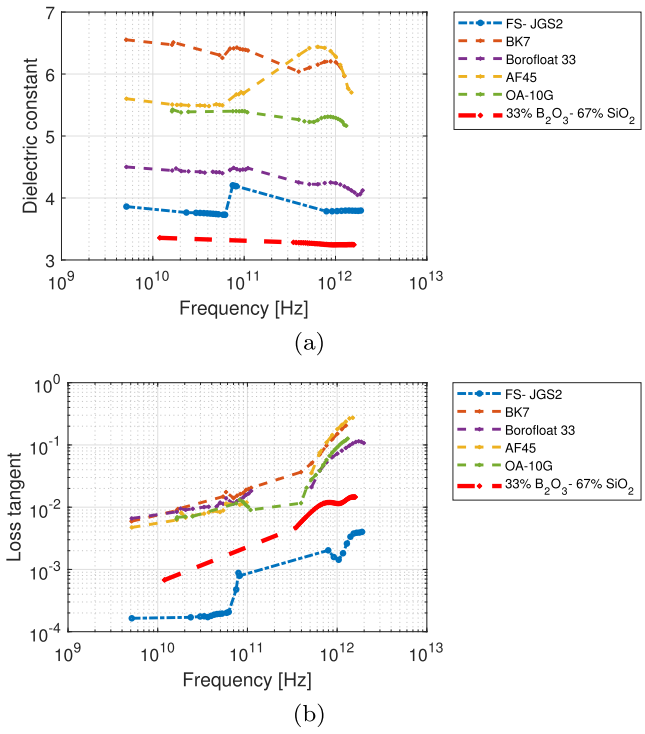

FIG. 3. (a) Dielectric constant comparison. (b) Loss tangent comparison.

amount of boron oxide in the measured composition due to the lower overall mass of the sample. It is important to note that the processing temperature was 1600 °C, which is below the melting point of silica, contributing to the presence of unmelted material.

TABLE II. Measured borosilicate glass compositions from ICP analysis.

Batched composition	B_2O_3 (mol. %)	SiO_2 (mol. %)	Al_2O_3 (mol. %)	Fe_2O_3 (mol. %)
33% B_2O_3–67% SiO_2	48.72	51.01	0.161	0.022
60% B_2O_3–40% SiO_2	58.01	41.76	0.120	0.021
67% B_2O_3–33% SiO_2	57.70	42.01	0.124	0.035
90% B_2O_3–10% SiO_2	84.99	14.95	<0.001	0.017

Moreover, for the ICP sample of the 33% B_2O_3–67% SiO_2 glass, the tail from the pour was taken, which had less stones than the actual pour, where the dielectric measurements were performed.

To improve the processability and durability of this glass from hydration and corrosion,[8] a small percentage of alkali has been added to the borosilicate glass.[13,14] The relation between boron and silicon has been kept constant (50% B–50% Si, which corresponds to 33% B_2O_3–67% SiO_2). The dielectric properties of the different alkali borosilicate glasses are given in Table III. There is a monotonic increment of the dielectric loss, as the alkali percentage increases. However, the loss tangent values of 2% and 5% mol alkali oxide are still low enough for the desired application. When 10 mol. % of alkali oxide is added, there is around an order of magnitude change in the loss compared to the 33% B_2O_3–67% SiO_2 composition. With the alkali addition, the lower hydration was indicated by the clarity of the glass after months.

We propose a metric to assess the loss of a glass in terms of polarizability. As mentioned earlier, the polarizability of a non-crystalline compound is higher than the one of its crystalline counterparts. We define the polarizability increment as the percentage rise in polarizability from an ideal crystalline phase to amorphous. For each composition, it is necessary to calculate the polarizability as if the compound provided an ideal crystalline material and the polarizability of the resulting glass (see Ref. 6 for more details). For the ideal crystalline part, the polarizabilities of all the ions are added together.[7] In the amorphous case, the dielectric properties and the density need to be measured. Then, Eq. (1) allows us to obtain the polarizability. The polarizability increment, $\Delta\alpha$, can be calculated as

$$\Delta\alpha = \frac{\alpha_G - \alpha_X}{\alpha_X} \cdot 100, \tag{3}$$

where α_G is the polarizability of the glass and α_X is the polarizability of the ideal crystalline counterpart. For instance, from Ref. 7, the ion dielectric polarizabilities of B, O, and Si are 0.05, 2.01, and 0.87, respectively. To obtain the ideal crystalline polarizability of 33% B_2O_3–67% SiO_2, $\alpha_X = 0.33 \cdot (0.05 \cdot 2 + 2.01 \cdot 3) + 0.67 \cdot (0.87 + 2.01 \cdot 2) = 5.29$. To obtain the glass polarizability of 33% B_2O_3–67% SiO_2, the values of $\epsilon_r = 3.47$ and $\rho = 2.0468$ are needed instead. From Eq. (1), $\alpha_G = 5.529$.

Figure 4 shows the loss tangent as a function of the glass polarizability increment from an ideal crystalline to a glassy state. The loss tangent values shown in Fig. 4 are for single phase pure fused silica and immiscible multiphase borosilicate glass systems. Since the phase distribution and volume of each phase in the immiscible microstructures are significantly smaller than the electromagnetic wavelength, the dielectric properties can be averaged according to effective medium theory. In this instance, the increment in polarizability is a result of the specific surroundings of each cation within the glass structure, irrespective of the specific cation present in each individual phase.

In this study, binary alkali silicates have also been added for comparison, and they are labeled as [Li, Na, K]y, with y being the alkali oxide mol percentage. Several commercial glasses have also been included: AF45, OA10G, BK7, and Borofloat 33 (BF33). The dielectric constant of these samples in the 16–18 GHz range is 5.5, 5.4, 6.5, and 4.4, respectively.[12] From Fig. 4, it is possible to see that the borosilicate composition labeled as BS (33% B_2O_3–67% SiO_2) has a polarizability increment smaller than fused silica, which

TABLE III. Dielectric properties and density of the manufactured glasses.

Name	Composition (mol. %)	Permittivity	Loss tangent	Density
BS	33% B_2O_3–67% SiO_2	3.470	6.540×10^{-4}	2.046
Li2BS	2% Li_2O–32.34% B_2O_3–65.66% SiO_2	3.808	1.119×10^{-3}	2.076
Li5BS	5% Li_2O–31.35% B_2O_3–63.65% SiO_2	3.984	2.415×10^{-3}	2.094
Li10BS	10% Li_2O–29.7% B_2O_3–60.3% SiO_2	4.456	4.212×10^{-3}	2.170
Na2BS	2% Na_2O–32.34% B_2O_3–65.66% SiO_2	3.846	1.380×10^{-3}	2.053
Na5BS	5% Na_2O–31.35% B_2O_3–63.65% SiO_2	4.128	3.580×10^{-3}	2.113
Na10BS	10% Na_2O–29.7% B_2O_3–60.3% SiO_2	4.463	4.126×10^{-3}	2.168
K2BS	2% K_2O–32.34% B_2O_3–65.66% SiO_2	3.935	1.951×10^{-3}	2.064
K5BS	5% K_2O–31.35% B_2O_3–63.65% SiO_2	4.110	3.595×10^{-3}	2.110
K10BS	10% K_2O–29.7% B_2O_3–60.3% SiO_2	4.487	6.691×10^{-3}	2.167

explains why its loss tangent is so low. Adding a small percentage of alkali to the borosilicate glass increases the polarizability around 5%, but it does not increase the loss tangent considerably. A roughly linear relationship between polarizability increment and loss tangent can be observed.

An interesting observation from Fig. 4 is that the introduction of alkali modifiers to fused silica (FS) results in a much larger increase in the loss tangent compared to a similar increase in the polarizability increment when the same alkali modifiers are added to the borosilicate (BS). This observation also extends to comparing the ternary alkali borosilicates to the binary alkali silicates. While both systems are known to possess nanoscale-or-larger phase separation[15] (Chap. 4), alkali borosilicates separate into modifier-borate rich and silica-rich regions, while alkali silicates separate into modifier-rich and silica-rich regions. The lack of an increase in loss tangent when small amounts of modifier are added to a borosilicate glass may be due to the formation of four-coordinated boron units within the phase separated regions instead of non-bridging oxygens. According to Ref. 16 (Chap. 7.4), in the region of the ternary Na_2O–B_2O_3–SiO_2 with a lower silica content, the droplets are a SiO_2-rich phase embedded in an alkali-rich borate matrix. Future work directly connecting the boron coordination within these phase separated regions to dielectric properties, as well as the local phase composition, may further elucidate this possible connection.

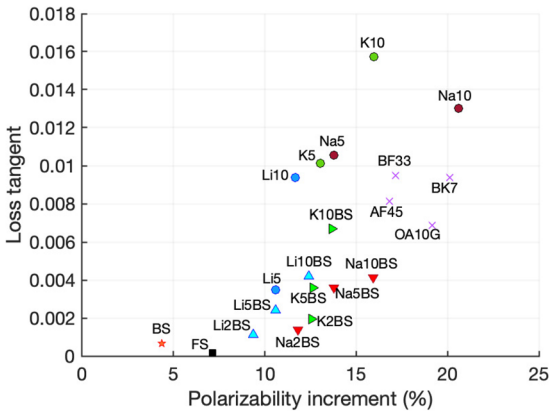

FIG. 4. Loss tangent as a function of the polarizability increment of the glassy state compared to the crystalline one. The dielectric properties have been measured in the K_u band. The borosilicates (BS) are the work of the current paper.

IV. CONCLUSIONS

The combination of silica and boron oxide results in a phase-separated microstructure that exhibits a significantly lower dielectric constant and loss compared to any commercially available glasses within the mm-wave to THz frequency range. The confirmation of immiscibility through energy dispersive spectroscopy further solidifies the innovative contributions of this research. The implications of these findings extend beyond theoretical considerations, offering a promising avenue for the development of advanced materials with enhanced dielectric properties for packaging applications in the chips for the next generation of communications. The susceptibility of boron to water could be advantageous for the etching of vias in the glass interposer, facilitating more precise and efficient material removal during the fabrication process. Vias are essential in an interposer as they provide crucial electrical interconnections in systems-on-package. The samples with a higher boron oxide content led to higher viscosity, making it challenging to pour the molten material. While the addition of alkalis lowered viscosity, additional research is necessary to achieve the production of thin laminates with a thickness less than a millimeter.

A metric has also been proposed to relate the dielectric properties to the material internal structure, which helps with the development of low loss materials.

ACKNOWLEDGMENTS

This work was supported, in part, by the National Science Foundation as part of the Center for Dielectrics and Piezoelectrics under Grant Nos. IIP-1841453 and IIP-1841466 and by a research Grant No. 41389 from VILLUM FONDEN. The authors thank Ling Cai and Nicholas Smith for providing the single alkali silicate samples.

AUTHOR DECLARATIONS

Conflict of Interest

The authors have no conflicts to disclose.

Author Contributions

Rocio Rodriguez-Cano: Data curation (lead); Investigation (equal); Writing – original draft (lead). **Nicholas L. Clark**: Investigation (equal). **John C. Mauro**: Investigation (equal). **Michael T. Lanagan**: Conceptualization (equal); Investigation (equal); Resources (lead); Writing – review & editing (equal).

DATA AVAILABILITY

The data that support the findings of this study are available from the corresponding author upon reasonable request.

REFERENCES

[1]M. Swaminathan, M. Kathaperumal, K.-S. Moon, H. Sharma, P. Murali, and S. Ravichandran, "Materials for heterogeneous integration," MRS Bull. **46**, 967–977 (2021).
[2]S. Ravichandran, K.-Q. Huang, M. Rehman, S. Erdogan, A. Watanabe, N. Nedumthakady, F. Liu, M. Kathaperumal, and M. Swaminathan, "Packaging approaches for mm wave and sub-THz communication," in *2019 IEEE MTT-S International Microwave Conference on Hardware and Systems for 5G and Beyond (IMC-5G)* (IEEE, 2019), pp. 1–5.
[3]L. Brusberg, H. Schroder, M. Topper, and H. Reichl, "Photonic system-in-package technologies using thin glass substrates," in *2009 11th Electronics Packaging Technology Conference* (IEEE, 2009), pp. 930–935.
[4]X. Jia, X. Li, K.-S. Moon, and M. Swaminathan, "Die-embedded glass packaging for 6G wireless applications," MRS Adv. **7**, 630–634 (2022).
[5]S. Ravichandran, S. Yamada, T. Ogawa, T. Shi, F. Liu, V. Smet, V. Sundaram, and R. Tummala, "Design and demonstration of glass panel embedding for 3D system packages for heterogeneous integration applications," J. Microelectron. Electron. Packag. **16**, 124 (2018).
[6]M. T. Lanagan, L. Cai, L. A. Lamberson, J. Wu, E. Streltsova, and N. J. Smith, "Dielectric polarizability of alkali and alkaline-earth modified silicate glasses at microwave frequency," Appl. Phys. Lett. **116**, 222902 (2020).
[7]R. D. Shannon, "Dielectric polarizabilities of ions in oxides and fluorides," J. Appl. Phys. **73**, 348–366 (1993).
[8]L. Van Uitert, D. Pinnow, J. Williams, T. C. Rich, R. Jaeger, and W. Grodkiewicz, "Borosilicate glasses for fiber optical waveguides," Mater. Res. Bull. **8**, 469–476 (1973).
[9]M. E. Nordberg, "Properties of some Vycor-brand glasses," J. Am. Ceram. Soc. **27**, 299–305 (1944).
[10]M. Letz, H. Engelmann, G. Lautenschläger, N. Brune, X. Bai, B. Salski, and T. Karpisz, "Special glass for packaging of high frequency electronics," in *2021 51st European Microwave Conference (EuMC)* (IEEE, 2022), pp. 103–106.
[11]R. Charles and F. Wagstaff, "Metastable immiscibility in the B_2O_3–SiO_2 system," J. Am. Ceram. Soc. **51**, 16–20 (1968).
[12]R. Rodriguez-Cano, S. E. Perini, B. M. Foley, and M. Lanagan, "Broadband characterization of silicate materials for potential 5G/6G applications," IEEE Trans. Instrum. Meas. **72**, 1–8 (2023).
[13]P. Adams and D. Evans, "Chemical durability of borate glasses," in *Borate Glasses: Structure, Properties, Applications* (Springer, 1978), pp. 525–537.
[14]M. Velez, H. L. Tuller, and D. R. Uhlmann, "Chemical durability of lithium borate glasses," J. Non-Cryst. Solids **49**, 351–362 (1982).
[15]O. V. Mazurin and E. Porai-Koshits, *Phase Separation in Glass* (Elsevier, 1984).
[16]W. Vogel, "Historical development of glass chemistry," in *Glass Chemistry* (Springer, 1994), pp. 1–21.